RSC Advances

PAPER

View Article Online
View Journal | View Issue

Cite this: *RSC Adv.*, 2025, **15**, 50682

Atrazine degradation by aqueous ferrate(VI) activated with sulfite *vs.* thiosulfate: performance, products, and pathways

Qin Guo,[a] Chaoting Guan, *[bc] Yi Yang,[c] Yang Zhou[a] and Jin Jiang *[a]

Sulfur-reductants (*e.g.*, sulfite and thiosulfate) can enhance ferrate (Fe(VI)) oxidation toward organic contaminants, which has recently attracted increasing attention. This work presented a systematic and comparative study on the oxidation performance, products, and pathways of atrazine (ATZ, one of the most widely used *s*-triazine herbicides) by Fe(VI)/sulfite and Fe(VI)/thiosulfate systems. Both systems achieved efficient ATZ degradation with the optimal efficiency at neutral pH, and the efficiency was affected by reagents dosage and co-existing components (*e.g.*, Cl^-, NO_2^-, natural organic matter). Five oxidation products of ATZ were produced in Fe(VI)/sulfite and Fe(VI)/thiosulfate systems, and their formation was quantified. ATZ degradation was initiated *via* electron transfer, resulting in dealkylation, alkylic-oxidation, and dechlorination-hydroxylation. Specifically, the molar ratio of two primary products (atrazine amide (CDIT) and deethyl-atrazine (DEA)) was calculated. In Fe(VI)/sulfite system, the [CDIT]/[DEA] value varied in the range of 0.04–0.82, depending on solution chemistry. Comparatively, the ratio obtained in Fe(VI)/thiosulfate system kept relatively constant at ~0.2 under various conditions, coinciding with that reported in pure Fe(IV) oxidation. This discrepancy was attributed to the difference of reactive oxidants involved in Fe(VI)/sulfite ($SO_4^{\bullet-}$ and Fe(V)/Fe(IV)) *vs.* Fe(VI)/thiosulfate systems (Fe(IV) alone). These insights advance understanding of the novel Fe(VI)/sulfur-reductants systems, and promote their potential applications.

Received 13th October 2025
Accepted 9th December 2025

DOI: 10.1039/d5ra07813j

rsc.li/rsc-advances

1. Introduction

Rapid industrialization and urbanization are resulting in the discharge of a substantial amount of emerging organic chemicals into the aquatic environment, which has been a significant issue of global concern due to their adverse environmental and human health effects.[1,2] Consequently, it is imperative to develop green and efficient water purification methods for abatement of organic pollutants and controlling their toxicity. Among various water treatment reagents, ferrate ($Fe(VI)O_4^{2-}$, Fe(VI)) has attracted great attention in recent decades due to its multimodal action (*i.e.*, oxidation, disinfection, and coagulation) and environmentally friendly character.[3–6] Fe(VI) is a strong oxidizing agent with the redox potentials of +2.2 and +0.7 V (*vs.* NHE) in acidic and basic solutions, respectively. Fe(VI) has shown high effectiveness in degrading a wide range of organic pollutants, especially those containing electron-rich organic moieties (*e.g.*, phenols,[7,8] anilines,[9,10] amines[11,12] and olefins[13–15]). However, some recalcitrant pollutants (*e.g.*, triclocarban, caffeine, flumequine and trimethoprim) cannot be effectively transformed by Fe(VI).[13,16,17] Thus, many efforts have been paid to the activation of Fe(VI) by selectively producing high-valent iron species (*i.e.*, Fe(V)/Fe(IV)), which are known to be several orders of magnitude more reactive than Fe(VI).[17,18] Recent studies suggest that addition of sulfur-containing reductants such as bisulfite/sulfite (HSO_3^-/SO_3^{2-}) and thiosulfate ($S_2O_3^{2-}$) is a highly effective tool to improve the reactivity of Fe(VI).[13,19–23] In earlier studies, reactive radicals such as sulfate radical ($SO_4^{\bullet-}$), hydroxyl radical ($^{\bullet}OH$), and sulfite radial ($SO_3^{\bullet-}$), are proposed to dominate the enhanced oxidation of pollutants in the Fe(VI)/sulfite system.[22,23] However, later work reported that reactive Fe(V)/Fe(IV) intermediates were generated along with radicals (mainly $SO_4^{\bullet-}$) to participate in organics transformation and their relative contributions were dependent on solution chemistry (*e.g.*, the [Fe(VI)]/[sulfite] molar ratio, and solution pH).[13,20,21] By contrast, only high-valent iron species (mainly Fe(IV)) are involved in the Fe(VI)/thiosulfate system.[19,20] The discrepancy in Fe(VI) activation mechanism by sulfite *vs.* thiosulfate can be attributed to the fact that they are one-electron and two-electron transfer reductants respectively.[24–27]

[a]*Guangdong Basic Research Center of Excellence for Ecological Security and Green Development, Key Laboratory for City Cluster Environmental Safety and Green Development of the Ministry of Education, School of Ecology, Environment and Resources, Guangdong University of Technology, Guangzhou 510006, China. E-mail: jiangjinhit@126.com; jiangjin@gdut.edu.cn*

[b]*School of Environment and Civil Engineering, Dongguan University of Technology, Dongguan 523106, Guangdong, China. E-mail: guanct@gdut.edu.cn*

[c]*CAS Key Laboratory of Urban Pollutant Conversion, Department of Environmental Science and Engineering, University of Science and Technology of China, Hefei 230026, China*

Specifically, the reaction between sulfite and Fe(VI) is firstly *via* a one-electron transfer step yielding Fe(V) and $SO_3^{\bullet-}$ (eqn (1)), which undergo further transformation to form other reactive species such as Fe(IV) and $SO_4^{\bullet-}$ (eqn (2)–(5)).[13,19,20] Thiosulfate as a two-electron reductant reacts with Fe(VI) to produce Fe(IV) and $S_2O_4^{2-}$ (eqn (6)),[19] and Fe(IV) may solely contribute to organics degradation in Fe(VI)/thiosulfate system.[20] Overall, the novel Fe(VI)/sulfur-containing reductants system shows a good potential for application in enhanced water depollution due to the high oxidation efficiency,[28] little interference by water matrices (*e.g.*, chloride (Cl^-), carbonate/bicarbonate (CO_3^{2-}/HCO_3^-) and natural organic matter (NOM)), as well as the environmental friendliness of final reaction products (*e.g.*, $Fe(OH)_3$ and SO_4^{2-}).[29–33]

$$HFe^{VI}O_4^-/Fe^{VI}O_4^{2-} + SO_3^{2-} \rightarrow HFe^{V}O_4^{2-}/Fe^{V}O_4^{3-} + SO_3^{\bullet-} \quad (1)$$

$$HFe^{VI}O_4^-/Fe^{VI}O_4^{2-} + SO_3^{\bullet-} \rightarrow HFe^{V}O_4^{2-}/Fe^{V}O_4^{3-} + SO_3 \quad (2)$$

$$HFe^{V}O_4^{2-}/Fe^{V}O_4^{3-} + SO_3^{\bullet-} \rightarrow HFe^{IV}O_4^{3-}/Fe^{IV}O_4^{4-} + SO_3 \quad (3)$$

$$SO_3^{\bullet-} + O_2 \rightarrow SO_5^{\bullet-} \quad (4)$$

$$SO_5^{\bullet-} + HSO_3^- \rightarrow SO_4^{\bullet-} + SO_4^{2-} + H^+ \quad (5)$$

$$HFe^{VI}O_4^- + S_2O_3^{2-} \rightarrow HFe^{IV}O_3^- + S_2O_4^{2-} \quad (6)$$

Atrazine (ATZ) is one of the most widely used *s*-triazine herbicides in agriculture, which has been frequently detected in surface and ground waters due to its high mobility, only moderate ability to adsorb onto soils, comparatively long half-life and poor biodegradability.[34–37] Over the past decades, great concerns have been raised about the high toxicity and endocrine disruption potentials of ATZ even at trace levels,[36,38–40] leading to a strong demand for efficient ATZ removal technologies from aquatic environments. Studies have reported that $^{\bullet}OH$ and $SO_4^{\bullet-}$ are able to degrade ATZ at high reaction rates of 2.4∼3.0 × 10^9 M^{-1} s^{-1} and 3 × 10^9 M^{-1} s^{-1}, respectively.[41,42] Recently, the fast transformation of ATZ by high-valent metal-oxo species such as Fe(IV)[43,44] and Mn(III)[45] is also confirmed. In addition to the difference in ATZ degradation kinetics, these reactive species exhibit distinct reaction mechanisms with ATZ, leading to significant variations in the formation and distribution of products. This is primarily attributed to their inherent nature and oxidative properties.[44,46] For instance, both $SO_4^{\bullet-}$ and $^{\bullet}OH$ can induce dealkylation (*i.e.*, deethylation and deisopropylation) of ATZ, resulting in formation of deethylatrazine (DEA) and deisopropylatrazine (DIA). $SO_4^{\bullet-}$ reacts mainly *via* the electron transfer pathway, causing a strong prevalence of deethylation of ATZ (*i.e.*, the DEA yield is significantly higher than DIA). By contrast, H-abstraction is the dominant mechanism in the reaction of $^{\bullet}OH$ with ATZ, and such a preference was insignificant (*i.e.*, the yields of DEA and DIA are comparable).

The degradation of ATZ by Fe(VI)/sulfite and Fe(VI)/thiosulfate systems has been found in two previous studies.[19,21] However, a systematical study on the oxidation efficiency, influencing factors, products formation, and reaction pathways of ATZ has not been conducted yet. These aspects hold significant importance for enhancing the understanding of the oxidative characteristics and mechanisms of the Fe(VI)/sulfur-containing reductants system and facilitating its potential applications. So, in this work, the oxidative transformation of ATZ by Fe(VI)/sulfite and Fe(VI)/thiosulfate systems was comparatively studied under various conditions (*e.g.*, solution pH, reagents concentration, and co-existing components). The main oxidation products of ATZ in both systems were identified and quantified, and the distribution of specific ATZ oxidation products was investigated. These results were compared with the previously reported oxidation processes (*e.g.*, $SO_4^{\bullet-}$, $^{\bullet}OH$, and aqueous Fe(IV)). The potential reaction pathways of ATZ in Fe(VI)/sulfite and Fe(VI)/thiosulfate systems were proposed accordingly.

2. Materials and methods

2.1. Materials

Potassium ferrate (K_2FeO_4, purity >90%) was synthesized following the procedure described in a study by Thompson *et al.*.[47] Fe(VI) stock solutions were freshly prepared by dissolving crystal K_2FeO_4 in borate buffer (pH 10) and standardized spectrophotometrically. ATZ, DIA, DEA, dimethyl sulfoxide (DMSO), and humic acid (HA) were obtained from Sigma-Aldrich. Sodium sulfite (Na_2SO_3) and sodium thiosulfate ($Na_2S_2O_3$) were purchased from Sinopharm Chemical Reagent Co., Ltd (Shanghai, China). Atrazine amide (CDIT) was synthesized by the approach proposed by Hapeman-Somich *et al.*,[48] which was briefly described in our previous study.[45] Acetonitrile and methanol of high performance liquid chromatography (HPLC) grade were supplied by TEDIA Co., Ltd. Other chemicals were acquired from Aladdin Chemical Reagent Co., Ltd (Shanghai, China). All reagents were of analytical grade or higher unless specifically noted. All solutions were prepared using deionized (DI) water (18.2 MΩ cm^{-1}) from a Milli-Q purification system. Stock solutions of Na_2SO_3 and $Na_2S_2O_3$ were prepared daily before experiments.

2.2. Experimental procedures

Batch experiments were carried out in 50 mL glass conical bottles under magnetic stirring and a water bath equipment was used to maintain the constant temperature (25 ± 1 °C). Typical reactions were initiated by simultaneously adding stock solutions of Fe(VI) (100 μM) and sulfite (0–500 μM)/thiosulfate (0–100 μM) into pH-buffered solutions containing ATZ (10 μM). Acetate and borate buffer (10 mM) were used for pH 5 and 6 and pH 7–10, respectively, and adjusted by H_2SO_4 and NaOH if necessary. No significant variation of pH values was observed during the reactions. The samples were withdrawn at predetermined time intervals, and immediately quenched with excess DMSO. Then, they were kept in the dark for 72 h to achieve complete conversion of ATZ degradation intermediates to final products before analyzed with HPLC or HPLC-MS/MS. All experiments were repeated independently in triplicates, and the average values with standard deviations were presented.

2.3. Analytical methods

The detection of ATZ was performed by a Waters 2695 HPLC coupled with a Waters 2998 diode array detector, and a Waters symmetry C18 column (250 × 4.6 mm, 5 μm) was employed for chromatographic separations. The detection wavelength was set at 230 nm. The mobile phase consisted of 30% methanol and 70% DI water (containing 0.1% acetic acid) at a flow rate of 1 mL min^{-1}. The degradation products of ATZ were analyzed by an Agilent 1260 HPLC coupled to an ABSciex QTrap 5500 MS with an electrospray ionization (ESI) source. The calibration curve of main oxidaion products CDIT and DEA was depicted in Fig. S1. The separations were performed with a Waters XBridge C18 column (3.0 × 100 mm, 2.5 μm particle size). The detailed analytical parameters were consistent with those used in our previous study.[44]

3. Results and discussion

3.1. Oxidation kinetics of ATZ by Fe(VI)/sulfite *versus* Fe(VI)/thiosulfate systems

3.1.1. Oxidation of ATZ by Fe(VI)/sulfite system. The oxidation of ATZ (10 μM) by Fe(VI) (100 μM) in the presence of different initial concentrations of sulfite (0–500 μM) was investigated at a wide pH range (5–10). As shown in Fig. S2, the loss of ATZ by Fe(VI) alone was negligible in 2 min over the investigated pH range, while the addition of sulfite accelerated the transformation of ATZ by Fe(VI) at each pH except 10. The reaction ended swiftly within 10 s and afterward ATZ was not further degraded by the Fe(VI)/sulfite system. The most significant enhancing effect of sulfite was observed at neutral pH. For instance, in the presence of 250 μM sulfite, 6.3 μM ATZ was removed within 2 min at pH 7, while the ATZ loss respectively decreased to 3.2 and 1.9 μM with pH increasing to 9 or decreasing to 5. The low efficiency of the Fe(VI)/sulfite system at higher pH might be related to the decrease of redox potential of Fe(VI), resulting in a slower reaction rate of Fe(VI) with sulfite to produce reactive intermediates.[22,49] The enhancing effect of sulfite almost disappeared as the pH rose to 10. In addition, the stability of Fe(VI) significantly decreased at lower pH due to its accelerated self-decay,[23,50] which could be the cause for less ATZ removal.

The effect of initial sulfite concentration ($[sulfite]_0$) on ATZ degradation by the Fe(VI)/sulfite system was investigated at each pH (Fig. 1a). At pH 6 and 7, the loss of ATZ increased gradually with $[sulfite]_0$ increasing from 50 to 250 μM, and then decreased as $[sulfite]_0$ further increased to 500 μM. At pH 8 and 9, the maximum loss of ATZ was also obtained at $[sulfite]_0$ = 250 μM, but the further increase of $[sulfite]_0$ had an insignificant effect on ATZ removal. Noting that the best performance of the Fe(VI)/sulfite system at pH 6–9 in this work was achieved at the [Fe(VI)]/[sulfite] molar ratio of 1 : 2.5, close to those reported in previous studies (*e.g.*, 1 : 2 or 1 : 4).[20,22] For one thing, Fe(VI) decomposition was enhanced when higher concentrations of sulfite were added, resulting in more reactive intermediates generation for ATZ oxidation. For another, excess sulfite could compete with ATZ for the reactive intermediates. So, the different effects of $[sulfite]_0$ on ATZ degradation observed at different pH might be related to the relative rate of reactive intermediates formation *vs.* consumption. Additionally, the degradation of ATZ at pH 5 was hardly influenced by $[sulfite]_0$, probably due to the fast self-decay of Fe(VI) that dominated the reaction.

Further, the effect of initial Fe(VI) concentration ($[Fe(VI)]_0$) on ATZ degradation by the Fe(VI)/sulfite system was investigated with a constant $[Fe(VI)]_0/[sulfite]_0$ molar ratio of 1 : 2.5 at pH 7. As seen in Fig. 1b, as the $[Fe(VI)]_0$ increased from 50 to 200 μM, the ATZ removal efficiency was enhanced from 40.4% to 76.7%. The loss of ATZ after 2 min was enhanced from 4.0 to 7.7 μM (Fig. S3). However, an increase in the $[Fe(VI)]_0$ also leads to the formation of a greater amount of ferric (Fe(III)) precipitates. Consequently, although a higher initial Fe(VI) concentration improves ATZ degradation, it necessitates a careful consideration of the associated risk of 'yellowish water' caused by the precipitated Fe(III).

3.1.2. Oxidation of ATZ by Fe(VI)/thiosulfate system. Similar to the case of sulfite, the addition of thiosulfate also promoted the transformation of ATZ by Fe(VI) at pH 5–8, and the maximum removal efficiency of ATZ was achieved at pH 7 (Fig. 2a). The enhancing effect of thiosulfate became negligible

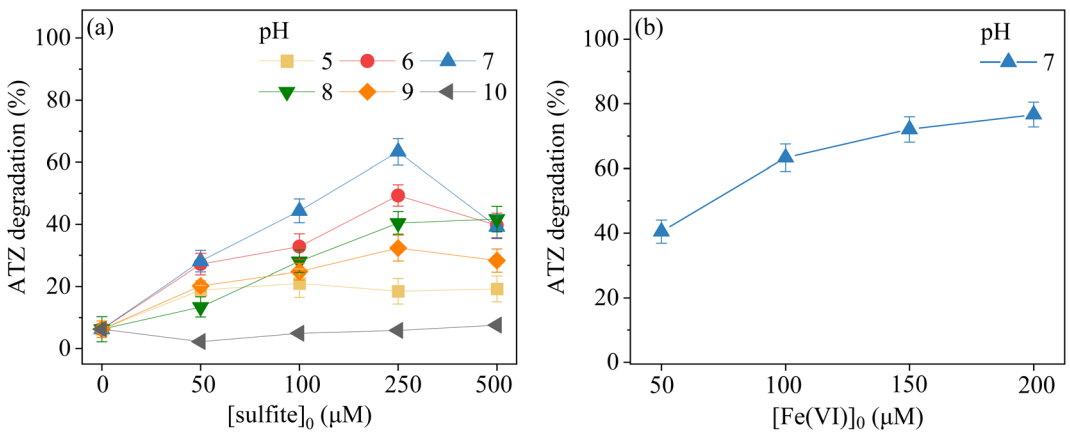

Fig. 1 The effects of pH and initial sulfite concentration (a) as well as initial Fe(VI) concentration (b) on ATZ degradation in Fe(VI)/sulfite system. Experimental conditions: $[ATZ]_0$ = 10 μM, $[Fe(VI)]_0$ = 50–200 μM, $[sulfite]_0$ = 0–500 μM, and pH = 5–10.

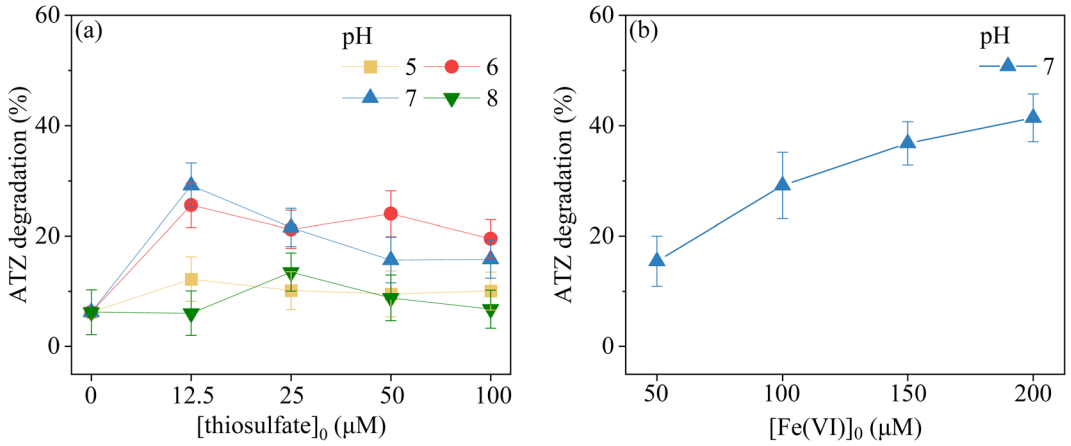

Fig. 2 The effects of pH and initial thiosulfate concentration (a) as well as initial Fe(VI) concentration (b) on ATZ degradation in Fe(VI)/thiosulfate system. Experimental conditions: $[ATZ]_0 = 10$ μM, $[Fe(VI)]_0 = 50–200$ μM, $[thiosulfate]_0 = 0–100$ μM, and pH = 5–8.

at higher pH (9 and 10, data not shown). The reaction was also quickly completed within 10 s, and then the concentration of ATZ remained unchanged (Fig. S4). The change of initial thiosulfate concentration ($[thiosulfate]_0$) showed different impacts on ATZ removal at different pH. At pH 5, similar extents of ATZ degradation (1.0–1.2 μM) were observed at the $[thiosulfate]_0$ range of 12.5–100 μM. At pH 6 and 7, the ATZ loss decreased from 2.6 and 3.0 μM to 1.7 and 1.5 μM with the increase of $[thiosulfate]_0$ from 12.5 to 100 μM. At pH 8, the ATZ loss firstly increased from 0.6 to 1.3 μM as $[thiosulfate]_0$ increased from 12.5 to 25 μM, and then decreased to 0.6 μM as $[thiosulfate]_0$ increased to 100 μM. Generally, addition of more thiosulfate was adverse to the degradation of ATZ in the Fe(VI)/thiosulfate system, consistent with the observation in the Fe(VI)/sulfite system. So, when sulfur-containing reductants are used to enhance the removal of pollutants by Fe(VI), their optimal dosages should be carefully adjusted according to actual solution conditions. The effect of $[Fe(VI)]_0$ on ATZ degradation by the Fe(VI)/thiosulfate system was investigated with the constant $[Fe(VI)]_0/[thiosulfate]_0$ molar ratio of 8 : 1 at pH 7. Similar to the case of the Fe(VI)/sulfite system, as the $[Fe(VI)]_0$ increased from 50 to 200 μM, the ATZ removal efficiency was enhanced from 15.5% to 41.4% (Fig. 2b). The loss of ATZ after 2 min was enhanced from 1.5 to 4.14 μM (Fig. S5).

3.1.3. Effect of water matrices. The impacts of water background matrices including Cl^-, CO_3^{2-}, sulfate (SO_4^{2-}), nitrate (NO_3^-), nitrite (NO_2^-) and NOM on ATZ degradation efficiency in Fe(VI)/sulfite and Fe(VI)/thiosulfate systems were evaluated, as displayed in Fig. 3a and b respectively. The presence of SO_4^{2-}, NO_3^-, and CO_3^{2-} showed a negligible effect on ATZ oxidation in both systems, while Cl^-, NO_2^-, and NOM had varying degrees of inhibitory effects. Compared with the control, the degradation efficiency of ATZ by Fe(VI)/sulfite system decreased from 63.7% to 25.7% due to the presence of 1 mM Cl^-. In the case of Fe(VI)/thiosulfate system, the value was decreased from 30.2% to 23.1%. The inhibitory effect of Cl^- on the Fe(VI)/thiosulfate system was weaker than that of the Fe(VI)/sulfite system, probably due to the discrepancy in main reactive species generated in two systems. It was reported that both $SO_4^{\bullet-}$ and Fe(V)/Fe(IV) were formed in Fe(VI)/sulfite system but high-valent iron species solely served as the oxidant in Fe(VI)/thiosulfate system.[19,20] $SO_4^{\bullet-}$ as a non-selective oxidant

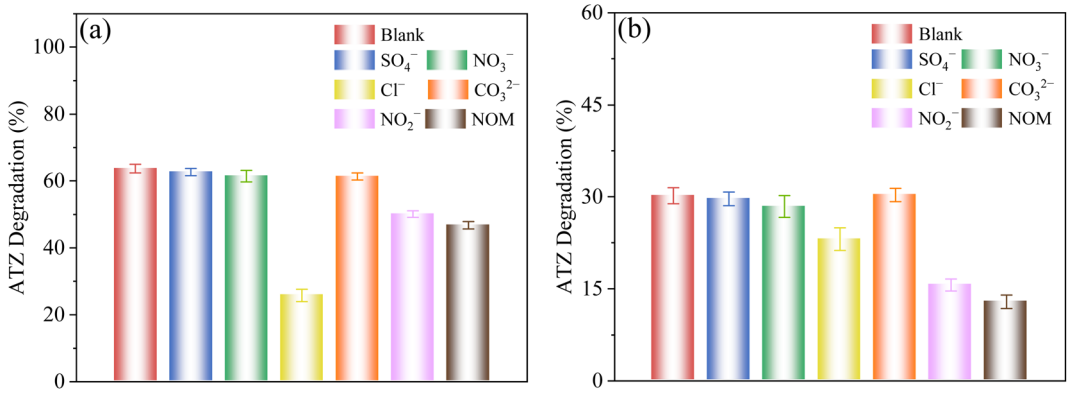

Fig. 3 The effect of water matrices on ATZ degradation in Fe(VI)/sulfite (a) and Fe(VI)/thiosulfate (b) systems. Experimental conditions: $[ATZ]_0 = 10$ μM, $[Fe(VI)]_0 = 100$ μM, $[sulfite]_0 = 250$ μM (a), $[thiosulfate]_0 = 12.5$ μM (b), pH = 7, $[Cl^-]_0 = [SO_4^{2-}]_0 = [NO_3^-]_0 = [CO_3^{2-}]_0 = 1$ mM, $[NO_2^-]_0 = 50$ μM, $[NOM]_0 = 10$ mg C per L, and reaction time of 2 min.

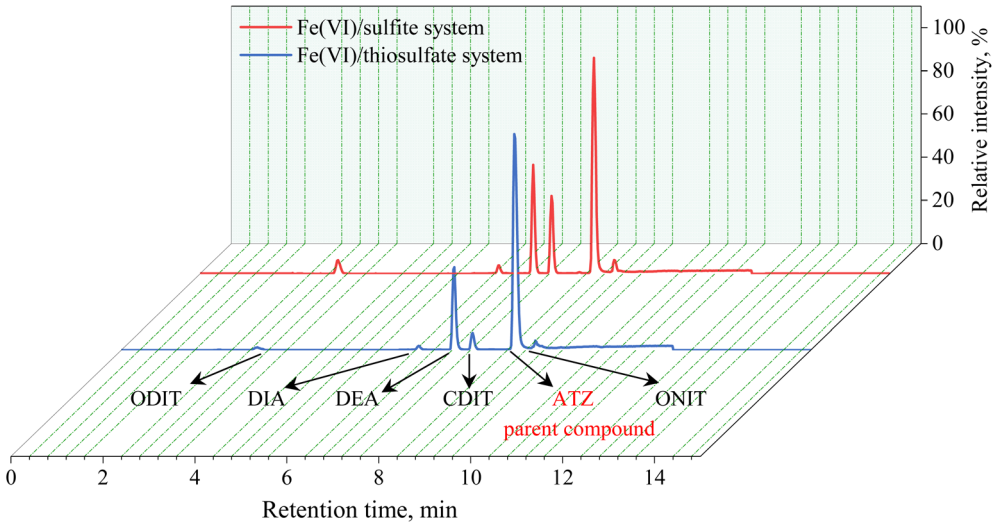

Fig. 4 HPLC/ESI- QTrap MS chromatogram of a sample containing ATZ treated by Fe(VI)/sulfite and Fe(VI)/thiosulfate system. Experimental conditions: $[ATZ]_0 = 10$ μM, $[Fe(VI)]_0 = 100$ μM, $[sulfite]_0 = 250$ μM (a), $[thiosulfate]_0 = 12.5$ μM (b), pH = 7, and reaction time of 2 min.

possesses quite high reactivity toward Cl^-, and thus is more easily captured by Cl^- compared to high-valent iron species.[20] By contrast, NO_2^- and NOM showed more significant inhibition on the Fe(VI)/thiosulfate system than the Fe(VI)/sulfite system.

To evaluate the practical applicability of the Fe(VI)/sulfur-containing reductants systems, ATZ degradation in secondary clarifier influent and surface water was compared with that in deionized water. Since the pH of the collected secondary clarifier influent and surface water samples ranged from 7.8 to 8.0, experiments in the deionized water were conducted at pH 8.0 (borate buffer) to maintain consistent conditions for comparison. As shown in Fig. S6, ATZ degradation efficiency in the two actual water samples was reduced in both Fe(VI)/sulfite (40.5% to 35.8% and 30.8%) and Fe(VI)/thiosulfate systems (29.2% to 26.6% and 25.4%). The Fe(VI)/thiosulfate system, however, was far less influenced, achieving a approximate ATZ degradation efficiency in secondary clarifier influent and surface water compared with that in deionized water.

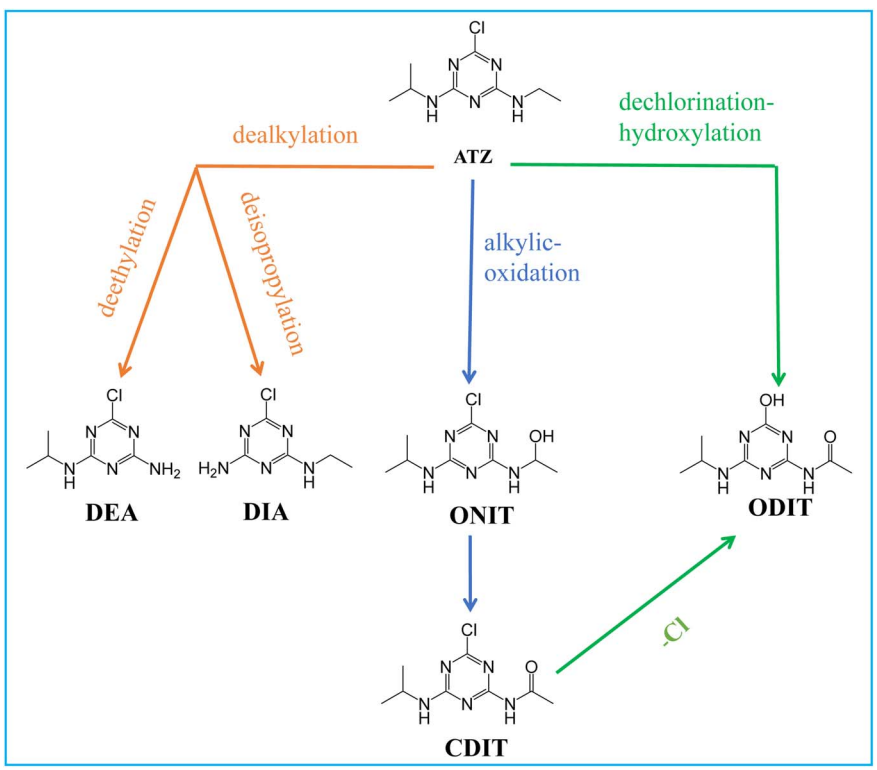

Scheme 1 Potential reaction pathways of ATZ in Fe(VI)/sulfur-containing reductants systems.

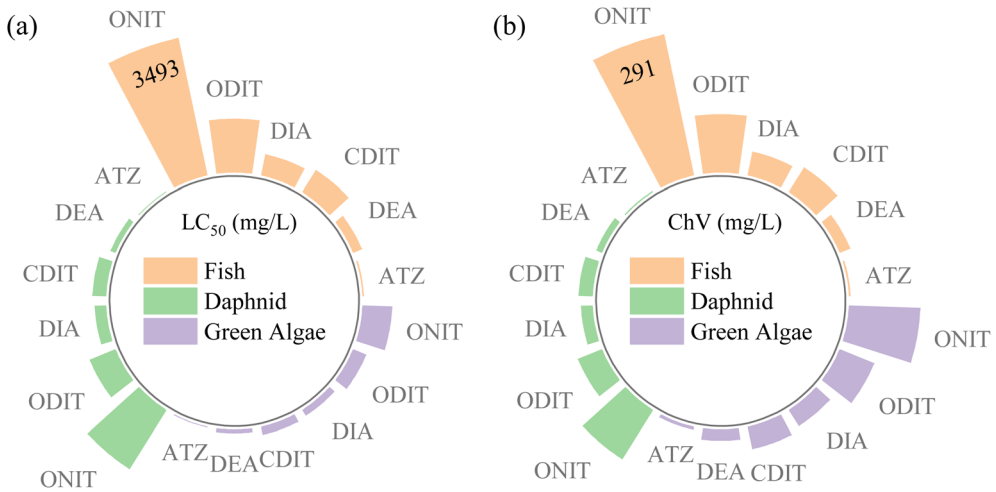

Fig. 5 Comparation of the LC_{50} (a) and ChV (b) of ATZ and its oxidation products in Fe(VI)/sulfur-containing reductants system.

3.2. ATZ oxidation products and reaction pathways

3.2.1. Identification and quantification of ATZ oxidation products. Oxidation products of ATZ formed in Fe(VI)/sulfite and Fe(VI)/thiosulfate systems were monitored by HPLC-MS/MS, and their structural identification was on the basis of their molecular weights, MSMS spectra, and standard substances. As shown in Fig. 4, the product retention times in the Fe(VI)/sulfite and Fe(VI)/thiosulfate systems are similar, while their response intensities differ. Detailed information on ATZ and its products (*e.g.*, retention times, molecular weights, and chemical structures) was presented in Table S1 and Fig. S7. In total, five major products were detected in both systems, including DIA, DEA, CDIT, *N*-(4-hydroxy-6-(isopropylamino)-1,3,5-triazin-2-yl) acetamide (ODIT), and 2-hydroxy-4-(2-hydroxy-ethylamino)-6-isopropylamino-*s*-triazine (ONIT).

Based on the identified products, the main transformation pathway of ATZ by Fe(VI)/sulfite and Fe(VI)/thiosulfate systems generally included dealkylation, alkylic-oxidation, dechlorination-hydroxylation (Scheme 1). Similar products were also observed in treatment of ATZ by other oxidation systems such as the Mn(IV)/sulfite system, O_3, Fe(II)/O_3 system, $^{\bullet}OH$, and/or $SO_4^{\bullet-}$ involved reactions, and the same reaction pathways were proposed.[35,41,42,44,45]

Moreover, five oxidation products of ATZ (10 μM) during treatment by Fe(VI)/sulfite (100/250 μM) and Fe(VI)/thiosulfate (100/12.5 μM) systems were quantified at pH 7. The selection of conditions was based on the maxima of ATZ removal and products formation. For the Fe(VI)/sulfite system, the products formation was in the following order: [DEA] (1.17 μM) > [CDIT] (0.45 μM) > [DIA] (0.2 μM) > [ODIT] (0.23 μM) > [ONIT] (0.01 μM). For the Fe(VI)/thiosulfate system, the order was as follows: [DEA] (0.60 μM) > [CDIT] (0.11 μM) > [DIA] (0.09 μM) > [ODIT] (0.04 μM) > [ONIT] (0.01 μM). In both systems, the production of products follows a consistent order, implying the similar reaction pathways for ATZ oxidation. Notably, since there are no standard substances for ONIT and ODIT, their nominal concentrations are approximated based on the response intensity of the CDIT standard, which shares a nearly identical structure. This method of estimation has been effectively utilized in previous studies.[44,45]

Furthermore, the toxicity of ATZ and its oxidation products was assessed using the ECOSAR V2.2 model, with the results presented in Fig. 5. The result revealed that the predicted median lethal concentrations (LC_{50}) and chronic toxicity values (ChV) for all major oxidation products were substantially higher than those of the parent ATZ for fish, daphnid, and green algae, indicating a significant reduction in both acute and chronic aquatic toxicity after treatment by the Fe(VI)/sulfur-containing reductants system. The toxicity of the oxidation products exhibited a distinct structure-dependent trend, with the dechlorinated-hydroxylated products (ODIT, ONTI) being the least toxic, followed by the alkyl-oxidation product (CDIT), while the dealkylated products (DEA, DIA) retained the highest residual toxicity. Comprehensive toxicological data was available in Table S2.

3.2.2. Reaction pathways. The quantification of ATZ oxidation products could give mechanistic insights into reactions of ATZ with the Fe(VI)/sulfite and Fe(VI)/thiosulfate systems (Scheme 1). For the dealkylation pathway, deethylation of ATZ was favored over deisopropylation in both systems, reflected by the much higher yield of DEA than DIA. The significant prevalence of deethylation suggested that electron transfer was the dominant pathway for ATZ dealkylation in both systems, which was consistent with the cases of ATZ oxidation by pure $SO_4^{\bullet-}$ or Fe(IV).[42,44] This result was quite reasonable since $SO_4^{\bullet-}$ and/or high-valent iron species were identified as the main oxidizing species in Fe(VI)/sulfur-containing reductants systems. For the alkylic-oxidation of ATZ, only products of ethyl group oxidation (*i.e.*, ONIT and CDIT) were observed while no products of isopropyl group oxidation were found in both systems. This might be attributed to the fact that the first step of ATZ alkylic-oxidation was initiated by electron transfer, favorable to the ethyl group hydroxylation to generate ONIT.[44] The subsequent H-abstraction of the hydroxylated ethyl group generated the carbonylation product CDIT. Noticeably, the yield of CDIT was

Table 1 A summary of the [CDIT]/[DEA] value obtained in ATZ transformation by various oxidation systems

Oxidation systems	Reactive species	[CDIT]/[DEA]	pH
UV/H_2O_2	$^{\bullet}OH$	~0.7[a,b]	3–9
UV/PDS	$SO_4^{\bullet-}$	~2.3[a,b]	3–9
Fe(II)/O_3	Fe(IV)	~0.2[a]	3–9
Mn(IV)/sulfite	$SO_4^{\bullet-}$, Mn(III)	3.0–4.0[b]	3
Fe(VI)/sulfite	$SO_4^{\bullet-}$, Fe(V)/Fe(IV)	0.04–0.82[c]	5–9
Fe(VI)/thiosulfate	Fe(IV)	~0.2[c]	5–8

[a] Data was obtained from the study by Guo *et al.*[44] [b] Data was obtained from the study by Guo *et al.*[45,46] [c] Measured by this study.

far greater than ONIT in both systems, indicating the fast transformation of ONIT to CDIT. Further, the resulting CDIT underwent dechlorination-hydroxylation to generate ODIT.

3.3. [CDIT]/[DEA] obtained in ATZ transformation by various oxidation systems

Due to the difference in the inherent nature and oxidative properties of various oxidants, they react with ATZ *via* different pathways, which thus results in the reactive oxidant nature-dependent distribution of specific ATZ oxidation products. These observations have been used as a diagnostic approach for distinguishing the role of reactive oxidants in various processes. For instance, the [DEA]/[DIA] value has been successfully applied to distinguish $^{\bullet}OH$ from $SO_4^{\bullet-}$, which is corresponding to nearly 2 and 10, respectively.[42,43,51] However, the [DEA]/[DIA] value may be not applicable for evaluating the reactive oxidants in specific circumstances, such as the case that the yield of DIA is extremely low. Because even small errors in the measurement of DIA generation can result in significant deviations reflected in the [DEA]/[DIA] value. Interestingly, our recent work found that CDIT and DEA were two main products from ATZ transformation by Mn(IV)/sulfite system, and their ratio (*i.e.*, [CDIT]/[DEA]) could be a good alternative to [DEA]/[DIA] in distinguishing the contribution of $SO_4^{\bullet-}$ and Mn(III) species.[45] The [CDIT]/[DEA] values obtained in pure $^{\bullet}OH$ and $SO_4^{\bullet-}$ systems were ~0.7 and ~2.3, respectively, while it was quantified to be 3.0–4.0 in the case of ATZ oxidation by Mn(IV)/sulfite system. The deviation of [CDIT]/[DEA] from 2.3 was attributed to the involvement of Mn(III). Furthermore, we monitored the products formation and distribution of ATZ during transformation by aqueous Fe(IV), generated from the Fe(II)/O_3 system.[44] It was found that ATZ was rapidly degraded by Fe(IV) at pH 3–9, meanwhile resulting in significant formation of CDIT and DEA. Intriguingly, the [CDIT]/[DEA] value maintained relatively constant at ~0.2 independent on solution pH. In these regards, the [CDIT]/[DEA] value could be employed as a sensitive probe for distinguishing the role of reactive metal-oxo (*e.g.*, Mn-oxo and Fe-oxo) intermediates from radicals. The currently available [CDIT]/[DEA] values in ATZ transformation by various oxidation systems were summarized in Table 1.

3.4. Comparison of [CDIT]/[DEA] in Fe(VI)/sulfite *versus* Fe(VI)/thiosulfate systems

Further, the distribution of two primary oxidation products of ATZ (*i.e.*, DEA and CDIT) was investigated and compared in Fe(VI)/sulfite and Fe(VI)/thiosulfate systems. Their concentrations were quantified under different conditions (*i.e.*, various pH and $[sulfite]_0$/$[thiosulfate]_0$), and presented in Fig. S8 and S9 respectively. In general, the variation trends of CDIT and DEA production with sulfite/thiosulfate concentrations are consistent with the degradation behavior of ATZ at each pH. For instance, the [CDIT] and [DEA] values in Fe(VI)/sulfite system at pH 7 reached the maximum at $[sulfite]_0$ = 250 μM (Fig. S8), corresponding to the maximum removal of ATZ (Fig. 1). Then, the resulting [CDIT]/[DEA] values were quantified, as shown in Fig. 6.

In the case of Fe(VI)/sulfite system, the [CDIT]/[DEA] value changed significantly with the variation of pH (Fig. 6a). Specifically, the [CDIT]/[DEA] value remained at ~0.82 at pH 5, independent on $[sulfite]_0$. At pH 6–9, there was a slight upward trend in [CDIT]/[DEA] values with the increase of $[sulfite]_0$. The [CDIT]/[DEA] value was within the range of 0.35–0.52, 0.27–0.38, 0.07–0.13 and 0.04–0.05 at pH 6, 7, 8, 9, respectively. Moreover, it was clear that the [CDIT]/[DEA] value gradually increased with the decrease of pH. As mentioned above, the [CDIT]/[DEA] value

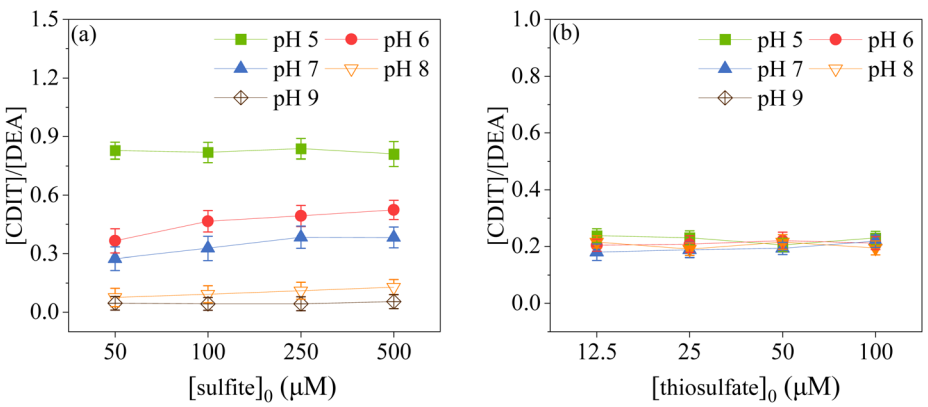

Fig. 6 The [CDIT]/[DEA] values obtained in ATZ degradation by Fe(VI)/sulfite (a) and Fe(VI)/thiosulfate (b) systems. Experimental conditions: $[ATZ]_0$ = 10 μM, $[Fe(VI)]_0$ = 100 μM, $[sulfite]_0$ = 50–500 μM (a), $[thiosulfate]_0$ = 12.5–100 μM (b), and reaction time of 2 min.

was ~2.3 and ~0.2 in the case of ATZ oxidation by pure $SO_4^{\bullet-}$ and Fe(IV) (Table 1). At pH 5–7, the [CDIT]/[DEA] values obtained in Fe(VI)/sulfite system were between 0.2 and 2.3, suggesting that both $SO_4^{\bullet-}$ and high-valent iron species were involved in ATZ transformation. With the decrease of pH and the increase of $[sulfite]_0$, [CDIT]/[DEA] gradually deviated from 0.2 and approached 2.3, indicating the enhanced contribution of $SO_4^{\bullet-}$. Interestingly, [CDIT]/[DEA] was lower than 0.2 at pH 8 and 9, probably related to the further transformation of CDIT by Fe(V). The major species of Fe(V) at pH 8–9 was $HFeO_4^{2-}$. It was documented that $HFeO_4^{2-}$ had higher reactivity toward some amino acids (*e.g.*, serine, glycine, and phenylalanine) than $H_2FeO_4^-$ and FeO_4^{3-}.[52] So, CDIT that contained a carbonyl group in its structure might be easily attacked by $HFeO_4^{2-}$, leading to the decrease of [CDIT]/[DEA] at pH 8–9. However, this hypothesis needs to be validated in future research by thoroughly studying the reaction pathways of Fe(V) with different structures of organic compounds. Moreover, these findings further confirmed that both $SO_4^{\bullet-}$ and high-valent iron species were produced in the Fe(VI)/sulfite system participating in transformation of ATZ and its oxidation products, in agreement with previous studies.[13,19,20]

Comparatively, the calculated [CDIT]/[DEA] value in Fe(VI)/thiosulfate system kept constant at ~0.2, independent of pH and $[thiosulfate]_0$ (Fig. 6b). This value well coincided with that obtained by pure Fe(IV), confirming the main role of Fe(IV) and negligible contribution of radicals in Fe(VI)/thiosulfate system. The significant discrepancy in the [CDIT]/[DEA] value obtained by Fe(VI)/sulfite *vs.* Fe(VI)/thiosulfate system again indicated the difference of Fe(VI) activation pathway as well as main reactive oxidants in two systems. Furthermore, it is noted that the involvement of Fe(V)/Fe(IV) in ATZ oxidation caused lower [CDIT]/[DEA] values compared to those obtained in pure $^{\bullet}OH$ or $SO_4^{\bullet-}$ oxidation (Table 1), suggesting that dealkylation was a preferred reaction pathway compared to alkylic-oxidation in reactions of high-valent iron species with ATZ.

4. Conclusions

This work demonstrated that sulfur-containing reductants including sulfite and thiosulfate could effectively activate Fe(VI) to enhance the degradation of ATZ, which was resistant to Fe(VI) alone. The degradation efficiency of ATZ was optimal at neutral pH, and was influenced by reagents dosage as well as the co-existing components. Similar oxidation products of ATZ were formed in Fe(VI)/sulfite and Fe(VI)/thiosulfate systems. Results of quantitative analysis of the products indicated that ATZ transformation by both systems was initiated by the electron transfer pathway, resulting in dealkylation, alkylic-oxidation, and dechlorination-hydroxylation of ATZ. Further, the molar ratio of two primary ATZ oxidation products CDIT and DEA was calculated under different conditions. During ATZ transformation by Fe(VI)/sulfite system, the [CDIT]/[DEA] value was variable in the range of 0.04–0.82 with the solution condition (*e.g.*, pH and $[sulfite]_0$). In contrast, the ratio remained constant at ~0.2 in the case of Fe(VI)/thiosulfate system, in good agreement with the value obtained by pure Fe(IV). This discrepancy in the [CDIT]/[DEA] value was attributed to the difference of primary reactive oxidants involved in Fe(VI)/sulfite *vs.* Fe(VI)/thiosulfate systems. These findings further improved the mechanistic understanding of the novel oxidation technology by combining Fe(VI) and sulfur-containing reductants. Moreover, the [CDIT]/[DEA] value in ATZ oxidation was highly dependent on the nature of reactive oxidants, which might thus be employed as a diagnostic approach for distinguishing the role of reactive species (*e.g.*, $^{\bullet}OH$, $SO_4^{\bullet-}$, and reactive metal-oxo intermediates) in various oxidation processes. However, this specific ratio might not serve as an indicator of changes in the toxicity of the transformation products, whereas the yield of dechlorination products might be more appropriate for the relevant assessment.

Author contributions

Qin Guo: writing – original draft, methodology, investigation, and data curation. Chaoting Guan: writing – review & editing, methodology, and validation. Yi Yang: methodology, project administration and resources, and supervision. Yang Zhou: investigation, project administration and resources, and data curation. Jin Jiang: project administration and resources, writing – review & editing, and supervision.

Conflicts of interest

There are no conflicts to declare.

Data availability

Access to the information that supports the current study will be provided at the official request.

Supplementary information (SI): additional details on the relative molecular mass and structure of the reaction products, the MSMS spectra and toxicity analysis of ATZ and its oxidation products, the detailed ATZ degradation by sulfite/thiosulfate system under various condition, the production of CDIT and DEA in ATZ degradation by Fe(VI) activated by sulfite/thiosulfate system. All data generated or analyzed during this study are included in this published article and its SI files. See DOI: https://doi.org/10.1039/d5ra07813j.

Acknowledgements

This work was financially supported by the program for Guangdong introducing innovative and entrepreneurial teams (2019ZT08L213), the National Natural Science Foundation of China (52200006, 42177045, 52470180, 52300015 and 42177004), the Anhui Provincial Natural Science Foundation (2208085ME152), the Fundamental Research Funds for the Central Universities (WK2400000004).

References

1 J. Li, S. Pang, Z. Wang, Q. Guo, J. Duan, S. Sun, L. Wang, Y. Cao and J. Jiang, Oxidative transformation of emerging

organic contaminants by aqueous permanganate: Kinetics, products, toxicity changes, and effects of manganese products, *Water Res.*, 2021, **203**, 117513.
2 S. Wu, L. Shen, Y. Lin, K. Yin and C. Yang, Sulfite-based advanced oxidation and reduction processes for water treatment, *Chem. Eng. J.*, 2021, **414**, 128872.
3 V. K. Sharma, R. Zboril and R. S. V. Ferrates, Greener Oxidants with Multimodal Action in Water Treatment Technologies, *Acc. Chem. Res.*, 2015, **48**, 182–191.
4 S. Wang, B. Shao, J. Qiao and X. Guan, Application of Fe(VI) in abating contaminants in water: State of art and knowledge gaps, *Front. Environ. Sci. Eng.*, 2021, **15**, 80.
5 X. Zhao, Z. Huang, J. Chen, Y. Liu, H. He, C. Cui, J. Ma and L. Wang, Differential Impacts of Pyrophosphate on Ferrates (VI, V, and IV): Through Its Unique Inhibition to Identify Fe (V) Species, *Environ. Sci. Technol.*, 2025, **59**, 7768–7778.
6 Y. Song, S. Zhang, H. Shen, W. Qin, J. Jiang and J. Ma, Calcium hypochlorite-potassium ferrate synergy: A novel strategy for stabilizing Fe (VI) while enhancing coagulation for emerging contaminants removal in source water, *J. Water Process Eng.*, 2025, **77**, 108427.
7 X. Sun, Q. Zhang, H. Liang, L. Ying, M. Xiangxu and V. K. Sharma, Ferrate (VI) as a greener oxidant: Electrochemical generation and treatment of phenol, *J. Hazard. Mater.*, 2016, **319**, 130–136.
8 M. Feng, X. Wang, J. Chen, R. Qu, Y. Sui, L. Cizmas, Z. Wang and V. K. Sharma, Degradation of fluoroquinolone antibiotics by ferrate (VI): Effects of water constituents and oxidized products, *Water Res.*, 2016, **103**, 48–57.
9 S. Sun, Y. Liu, J. Ma, S. Pang, Z. Huang, J. Gu, Y. Gao, M. Xue, Y. Yuan and J. Jiang, Transformation of substituted anilines by ferrate (VI): Kinetics, pathways, and effect of dissolved organic matter, *Chem. Eng. J.*, 2018, **332**, 245–252.
10 H. Yu, Y. Tian, S. Wang, X. Ke, R. Li and X. Kang, Ferrate (VI) oxidation mechanism of substituted anilines: a density functional theory investigation, *ACS Omega*, 2021, **6**, 14317–14326.
11 V. Rougé, P. T. T. H. Nguyen, S. Allard and Y. Lee, Reaction of amino acids with ferrate (vi): Impact of the carboxylic group on the primary amine oxidation kinetics and mechanism, *Environ. Sci. Technol.*, 2022, **57**, 18509–18518.
12 N. Noorhasan, B. Patel and V. K. Sharma, Ferrate (VI) oxidation of glycine and glycylglycine: kinetics and products, *Water Res.*, 2010, **44**, 927–935.
13 M. Feng and V. K. Sharma, Enhanced oxidation of antibiotics by ferrate(VI)-sulfur(IV) system: Elucidating multi-oxidant mechanism, *Chem. Eng. J.*, 2018, **341**, 137–145.
14 B. Li, R. Guo, J. Tian, Z. Wang and R. Qu, New findings of ferrate (VI) oxidation mechanism from its degradation of alkene imidazole ionic liquids, *Environ. Sci. Technol.*, 2021, **55**, 11733–11744.
15 A. Islam, D. Jeon, J. Ra, J. Shin, T. Kim and Y. Lee, Transformation of microcystin-LR and olefinic compounds by ferrate (VI): Oxidative cleavage of olefinic double bonds as the primary reaction pathway, *Water Res.*, 2018, **141**, 268–278.
16 B. Yang, G. Ying, J. Zhao, S. Liu, L. Zhou and F. Chen, Removal of selected endocrine disrupting chemicals (EDCs) and pharmaceuticals and personal care products (PPCPs) during ferrate(VI) treatment of secondary wastewater effluents, *Water Res.*, 2012, **46**, 2194–2204.
17 V. K. Sharma, M. Feng, D. D. Dionysiou, H. Zhou, C. Jinadatha, K. Manoli, M. F. Smith, R. Luque, X. Ma and C. Huang, Reactive High-Valent Iron Intermediates in Enhancing Treatment of Water by Ferrate, *Environ. Sci. Technol.*, 2022, **56**, 30–47.
18 T. He, B. Zhou, H. Chen and R. Yuan, Degradation of organic chemicals in aqueous system through ferrate-based processes: A review, *J. Environ. Chem. Eng.*, 2022, **10**, 108706.
19 M. Feng, C. Jinadatha, T. J. McDonald and V. K. Sharma, Accelerated Oxidation of Organic Contaminants by Ferrate(VI): The Overlooked Role of Reducing Additives, *Environ. Sci. Technol.*, 2018, **52**, 11319–11327.
20 Y. Gao, Y. Zhou, S. Pang, Z. Wang, Y. Shen and J. Jiang, Quantitative evaluation of relative contribution of high-valent iron species and sulfate radical in Fe(VI) enhanced oxidation processes via sulfur reducing agents activation, *Chem. Eng. J.*, 2020, **387**, 124077.
21 B. Shao, H. Dong, B. Sun and X. Guan, Role of Ferrate(IV) and Ferrate(V) in Activating Ferrate(VI) by Calcium Sulfite for Enhanced Oxidation of Organic Contaminants, *Environ. Sci. Technol.*, 2019, **53**, 894–902.
22 S. Sun, S. Pang, J. Jiang, J. Ma, Z. Huang, J. Zhang, Y. Liu, C. Xu, Q. Liu and Y. Yuan, The combination of ferrate(VI) and sulfite as a novel advanced oxidation process for enhanced degradation of organic contaminants, *Chem. Eng. J.*, 2018, **333**, 11–19.
23 J. Zhang, L. Zhu, Z. Shi and Y. Gao, Rapid removal of organic pollutants by activation sulfite with ferrate, *Chemosphere*, 2017, **186**, 576–579.
24 S. Wang, Y. Deng, B. Shao, J. Zhu, Z. Hu and X. Guan, Three kinetic patterns for the oxidation of emerging organic contaminants by Fe (VI): The critical roles of Fe (V) and Fe (IV), *Environ. Sci. Technol.*, 2021, **55**, 11338–11347.
25 X. Zhang, M. Feng, C. Luo, N. Nesnas, C. Huang and V. K. Sharma, Effect of metal ions on oxidation of micropollutants by ferrate (VI): enhancing role of FeIV species, *Environ. Sci. Technol.*, 2020, **55**, 623–633.
26 J. Chen, N. Wu, X. Xu, R. Qu, C. Li, X. Pan, Z. Wei and Z. Wang, Fe (VI)-mediated single-electron coupling processes for the removal of chlorophene: a combined experimental and computational study, *Environ. Sci. Technol.*, 2018, **52**, 12592–12601.
27 T. Yang, J. Mai, H. Cheng, M. Zhu, S. Wu, L. Tang, P. Liang, J. Jia and J. Ma, UVA-LED-assisted activation of the ferrate (VI) process for enhanced micropollutant degradation: important role of ferrate (IV) and ferrate (V), *Environ. Sci. Technol.*, 2021, **56**, 1221–1232.
28 Y. Chu, M. Xu, X. Li, J. Lu, Z. Yang, R. Lv, J. Liu, L. Lv and W. Zhang, Oxidation of emerging contaminants by S (IV) activated ferrate: Identification of reactive species, *Water Res.*, 2024, **251**, 121100.

29 Y. Lee and U. Von Gunten, Oxidative transformation of micropollutants during municipal wastewater treatment: Comparison of kinetic aspects of selective (chlorine, chlorine dioxide, ferrateVI, and ozone) and non-selective oxidants (hydroxyl radical), *Water Res.*, 2010, **44**, 555–566.

30 L. Niu, J. Lin, W. Chen, Q. Zhang, X. Yu and M. Feng, Ferrate (VI)/periodate system: synergistic and rapid oxidation of micropollutants via periodate/iodate-modulated Fe (IV)/Fe (V) intermediates, *Environ. Sci. Technol.*, 2023, **57**, 7051–7062.

31 Z. Tang and Y. Deng, Revisiting Ferrate (VI) Activation: Why Enhanced Reactivity Undermines Disinfection, *Environ. Sci. Technol. Lett.*, 2025, **12**, 1095–1101.

32 Z. Tang and Y. Deng, Activation or Deactivation? Rethinking Ferrate (VI) Reactivity within a Broader Modulation Framework, *ACS ES&T Water*, 2025, **5**, 4928–4930.

33 Y. Ren, B. Tan, C. Liu, C. Ji, B. Lai, W. Zhang and J. Li, Iodate (V) activated ferrate (VI) for enhanced oxidation of micropollutants from water and sediment media, *Chem. Eng. J.*, 2024, **480**, 147811.

34 H. Chen, E. Bramanti, I. Longo, M. Onor and C. Ferrari, Oxidative decomposition of atrazine in water in the presence of hydrogen peroxide using an innovative microwave photochemical reactor, *J. Hazard. Mater.*, 2011, **186**, 1808–1815.

35 J. A. Khan, X. He, N. S. Shah, H. M. Khan, E. Hapeshi, D. Fatta-Kassinos and D. D. Dionysiou, Kinetic and mechanism investigation on the photochemical degradation of atrazine with activated H_2O_2, $S_2O_8^{2-}$ and HSO_5^-, *Chem. Eng. J.*, 2014, **252**, 393–403.

36 O. F. Sanchez, L. Lin, C. J. Bryan, J. Xie, J. L. Freeman and C. Yuan, Profiling epigenetic changes in human cell line induced by atrazine exposure, *Environ. Pollut.*, 2020, **258**, 113712.

37 Z. Yang, A. Yu, C. Shan, G. Gao and B. Pan, Enhanced Fe(III)-mediated Fenton oxidation of atrazine in the presence of functionalized multi-walled carbon nanotubes, *Water Res.*, 2018, **137**, 37–46.

38 J. Ali Khan, X. He, H. M. Khan, N. S. Shah and D. D. Dionysiou, Oxidative degradation of atrazine in aqueous solution by UV/H_2O_2/Fe^{2+}, UV/$S_2O_8^{2-}$/Fe^{2+} and UV/HSO_5^-/Fe^{2+} processes: A comparative study, *Chem. Eng. J.*, 2013, **218**, 376–383.

39 T. Hayes, K. Haston, M. Tsui, A. Hoang, C. Haeffele and A. Vonk, Atrazine-induced hermaphroditism at 0.1 ppb in American leopard frogs (Rana pipiens): laboratory and field evidence, *Environ. Health Perspect.*, 2003, **111**, 568–575.

40 Y. L. Phyu, M. S. J. Warne and R. P. Lim, Toxicity and bioavailability of atrazine and molinate to the freshwater shrimp (Paratya australiensis) under laboratory and simulated field conditions, *Ecotoxicol. Environ. Saf.*, 2005, **60**, 113–122.

41 J. L. Acero, K. Stemmler and U. von Gunten, Degradation Kinetics of Atrazine and Its Degradation Products with Ozone and OH Radicals: A Predictive Tool for Drinking Water Treatment, *Environ. Sci. Technol.*, 2000, **34**, 591–597.

42 H. V. Lutze, S. Bircher, I. Rapp, N. Kerlin, R. Bakkour, M. Geisler, C. von Sonntag and T. C. Schmidt, Degradation of Chlorotriazine Pesticides by Sulfate Radicals and the Influence of Organic Matter, *Environ. Sci. Technol.*, 2015, **49**, 1673–1680.

43 Z. Dong, C. Jiang, Q. Guo, J. Li, X. Wang, Z. Wang and J. Jiang, A novel diagnostic method for distinguishing between Fe(IV) and $^{\bullet}OH$ by using atrazine as a probe: Clarifying the nature of reactive intermediates formed by nitrilotriacetic acid assisted Fenton-like reaction, *J. Hazard. Mater.*, 2021, **417**, 126030.

44 Q. Guo, Z. Wang, S. Pang and J. Jiang, Kinetic and Mechanistic Insights into the Oxidative Transformation of Atrazine by Aqueous Fe(IV): Comparison with Hydroxyl and Sulfate Radicals, *ACS ES T Eng*, 2023, **3**, 1402–1412.

45 Q. Guo, C. Guan, L. Luo, Z. Wang, H. Pan and J. Jiang, New insights into atrazine degradation by the novel manganese dioxide/bisulfite system: Product formation and Mn reuse, *J. Clean. Prod.*, 2022, **368**, 133106.

46 Q. Guo, Y. Cao, J. Jiang and J. Li, Dual roles of Atrazine as An Organic Contaminant and Indicator of Intermediate Oxidants during Sulfite Activation of Permanganate, *J. Environ. Chem. Eng.*, 2025, 119432.

47 G. W. Thompson, L. T. Ockerman and J. M. Schreyer, Preparation and purification of potassium ferrate. VI, *J. Am. Chem. Soc.*, 1951, **73**, 1379–1381.

48 C. J. Hapeman-Somich, G. Zong, W. R. Lusby, M. T. Muldoon and R. Waters, Aqueous ozonation of atrazine. Product identification and description of the degradation pathway, *J. Agric. Food Chem.*, 1992, **40**, 2294–2298.

49 V. K. Sharma, Oxidation of Inorganic Compounds by Ferrate(VI) and Ferrate(V): One-Electron and Two-Electron Transfer Steps, *Environ. Sci. Technol.*, 2010, **44**, 5148–5152.

50 Y. Lee, R. Kissner and U. von Gunten, Reaction of Ferrate(VI) with ABTS and Self-Decay of Ferrate(VI): Kinetics and Mechanisms, *Environ. Sci. Technol.*, 2014, **48**, 5154–5162.

51 C. Luo, J. Jiang, C. Guan, J. Ma, S. Pang, Y. Song, Y. Yang, J. Zhang, D. Wu and Y. Guan, Factors affecting formation of deethyl and deisopropyl products from atrazine degradation in UV/H_2O_2 and UV/PDS, *RSC Adv.*, 2017, **7**, 29255–29262.

52 V. K. Sharma, Ferrate(VI) and ferrate(V) oxidation of organic compounds: Kinetics and mechanism, *Coord. Chem. Rev.*, 2013, **257**, 495–510.